

文章编号: 2024-0177 (2024) 00-0000-00

DOI: 10.14027/j.issn.1000-0550.2024.119

上扬子北缘晚二叠世吴家坪期海洋氧化还原环境重建

雍茹男^{1,2}, 孙诗^{1,2}, 陈安清^{1,2}, 侯明才^{1,2}, 李夔洲^{1,2}, 李乾^{3,4}, 黄光辉^{1,2}, 李雯^{1,2}, 解昊¹, 陈洪德^{1,2}

1. 油气藏地质及开发工程全国重点实验室, 成都理工大学, 成都 610059

2. 自然资源部深时地理环境重建与应用重点实验室, 成都理工大学, 成都 610059

3. 环境与资源学院, 西南科技大学, 四川绵阳 621010

4. School of Earth Environment, University of Leeds, Leeds UK LS2 9JT

摘要 【目的】瓜德鲁普末期生物灭绝之后, 生物多样性在晚二叠世开始逐步恢复增长, 进一步确定晚二叠世浅海氧化还原状态和演化规律, 有助于厘清该时期生物复苏与海洋氧化还原变化之间的关系。【方法】选取上扬子北缘具高分辨率时间框架约束的上寺剖面吴家坪阶地层作为研究对象, 开展了沉积学和沉积地球化学研究, 重建了晚二叠世吴家坪期海洋氧化还原环境。【结果】碳酸盐岩铈异常指标和碳同位素在吴家坪期均呈现显著变化, 其中碳同位素的正偏和负偏分别对应于晚古生代P4冰期的形成与消融。吴家坪早期生物逐渐复苏导致海洋初级生产力提高和光合作用增强, 同时凉爽气候利于洋流循环和氧气交换, 该时期整体处于贫氧—氧化环境; 吴家坪中期开始, 随着气候转暖和晚古生代冰期消亡, 海洋通风减弱和海平面上升共同驱动最小含氧带的显著扩张, 海洋转变为缺氧环境。【结论】研究重建了晚二叠世吴家坪期浅海环境的氧化还原结构, 揭示了晚二叠世海洋缺氧与同期气候—构造事件的深层联系。

关键词 晚二叠世; Ce异常; 海洋缺氧; 生物复苏; 上扬子

第一作者简介 雍茹男, 女, 1999年出生, 硕士研究生, 地质学, E-mail: yongrunan@stu.cdut.edu.cn

通信作者 孙诗, 男, 研究员, 硕士生导师, 沉积学, E-mail: sstopwin@163.com

中图分类号 文献标志码 A

0 引言

晚二叠世是地球历史中的一个关键转折时期, 见证了一系列重大生物—环境地质事件: 泛大陆的裂解^[1-2], 晚古生代冰期的结束^[3-4], 西伯利亚大火成岩省的喷发^[5-6], 碳循环的强烈扰动^[7-8], 极热气候事件的出现^[9-10]以及二叠纪末生物大灭绝^[11-12]。该时期的生物演化与环境变化密切相关, 两者之间的相互作用机制已成为深时地球表层系统的研究热点^[13-14]。

海洋生物演化与海水氧化还原条件密切相关^[15-16], 通常氧化环境有利于生物繁衍, 缺氧环境不利于生物演化, 更为严重的缺氧硫化则直接威胁到生物生存^[17-18]。浅海是海洋生物的主要栖息地, 重建其氧化还原条件对全面理解海洋环境变化和生物演化之间的联系至关重要^[19-20]。晚二叠世吴家坪期是瓜德鲁普晚期生物灭绝之后的生物复苏时期, 尽管针对

收稿日期: 2024-10-09; **收修改稿日期:** 2024-11-12

基金项目: 国家自然科学基金项目(42402120, 42272132); 成都理工大学优质青年人才培育特支计划(20200-000526-04); 成都理工大学珠峰科学研究中心(80000-2024ZF11402) [Foundation: National Natural Science Foundation of China, No. 42402120, 42272132; Special Support Program for Cultivating High Quality Young Talents of Chengdu University of Technology, No. 20200-000526-04; Everest Scientific Research Program of Chengdu University of Technology, No. 80000-2024ZF11402]

该时期沉积环境、生物演化及气候变化已开展大量研究^[7,21-22], 但大多聚焦于该时期深水氧化还原状态对地质事件的响应, 对于该时期浅海水体的氧化还原条件的具体变化过程及驱动机制, 仍缺乏明确的认识。

华南板块在晚二叠世保存有完整海相沉积记录^[22-23], 位于扬子北缘的上寺剖面, 是华南二叠系研究程度较高的典型剖面之一^[7,24]。该剖面上二叠统地层受牙形石生物地层^[25]和凝灰岩放射性同位素年龄^[11]的双重时间约束, 为研究该时期古海洋环境变化提供了精确的年代地层框架。前人在该剖面开展了碳酸盐岩同位素和元素地球化学研究^[7,25], 但针对古海洋氧化还原条件方面的研究相对较少。碳酸盐岩稀土元素特征已广泛应用于重建地质历史时期海水的化学组成, 特别是铈异常 (Ce^*) 不易受到早期成岩作用的影响^[26-27], 可以作为示踪浅海氧化还原条件的绝佳指标^[28-29]。

本研究聚焦于华南上扬子北缘的上寺剖面, 针对上二叠统吴家坪阶地层开展沉积学和沉积地球化学研究。基于前人建立的高分辨率时间地层框架, 利用碳酸盐岩 Ce 异常指标, 重建了晚二叠世吴家坪期浅海环境的氧化还原演化过程。同时汇总同期相关生命环境指标, 进一步探讨该时期的碳循环波动、氧化还原条件及其与气候—构造事件之间的深层联系。

1 地质背景

二叠纪时期, 华南板块位于低纬度赤道附近(图 1a), 北部、西部和南部均被古特提斯洋围绕, 而东部毗邻泛大洋的深海盆地^[7,30-31], 是古特提斯多岛洋体系的一部分^[32-33]。中二叠世末期, 峨眉山大火成岩省喷发使得在扬子西缘中二叠统茅口组之上覆盖了巨厚峨眉山玄武岩^[13,34-35], 同时康滇古陆迅速抬升, 导致上扬子地区呈现为西高东低古地貌格局。随着吴家坪早期再次海侵和扬子北部勉略洋俯冲^[36-37], 该时期古地理分异度最为强烈(图 1), 从西向东依次发育陆相(宣威组)—海陆过渡相(龙潭组)—海相(吴家坪组)的沉积相带^[30,38-39]。

上寺剖面($32^{\circ}19'N$, $105^{\circ}27'E$)位于四川广元剑阁县上寺镇往北几百米处的长江沟边(图 1c), 是华南二叠系研究程度较高的典型剖面。剖面沿长江沟发育二叠纪海相碳酸盐岩地层, 地层序列由下往上依次为栖霞组、茅口组、吴家坪组和大隆组。本次研究的吴家坪组地层主要沉积于上扬子浅水台地到深水盆地的过渡相带(图 1b), 从大隆组沉积期开始沉积水体显著加深。Yuan *et al.*^[25]对该剖面上二叠统地层开展牙形刺化石带的鉴定, 其中吴家坪阶由吴家坪组和大隆组下部组成(图 1d), 吴家坪组对应吴家坪早中期, 建立了 2 个牙形带(*C. dukouensis*, *C. asymmetrica*), 大隆组下部对应吴家坪阶晚期, 建立了 3 个牙

形带 (*C. liangshanensis*, *C. transcaucasica*, *C. orientalis*)。此外, 该剖面上二叠统地层发育数层火山灰, 前人对其进行高精度的 U-Pb 定年^[11,40]。因此, 上寺剖面的高分辨率生物地层与同位素年代学为本次研究提供了很好的时间约束。

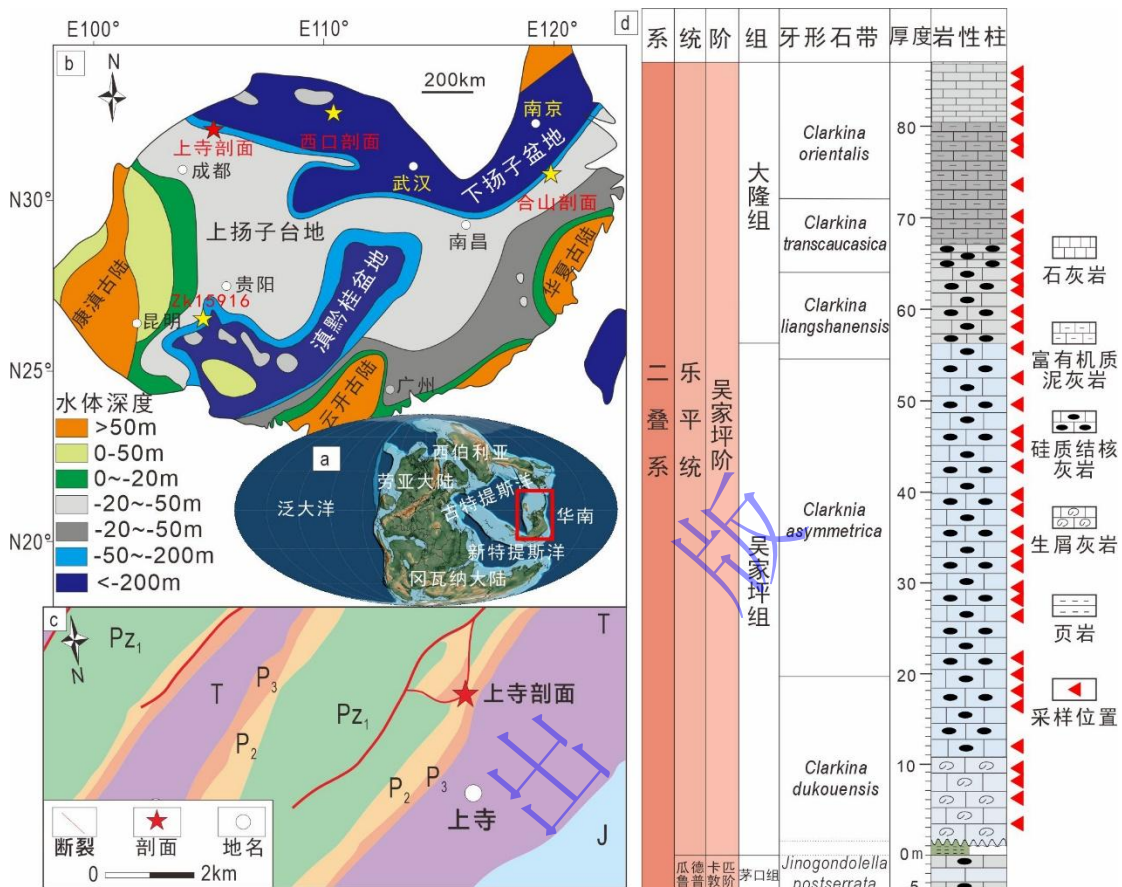


图 1 研究区地质背景

(a) 晚二叠世全球板块重建^[30]; (b) 晚二叠世华南岩相古地理^[25]; (c) 研究区地质图 (J.侏罗纪地层, T.三叠纪地层, P₃.上二叠统地层, P₂.中二叠统地层, P_{z1}.早古生界地层); (d) 上寺剖面岩石—生物地层序列^[25]

Fig.1 Geological setting of the study area

(a) Late Permian global plate reconstruction map^[30]; (b) Late Permian paleogeographic map of South China^[25]; (c) Geological map of the study area (J. Jurassic, T. Triassic, P₃. Upper Permian, P₂. Middle Permian, and P_{z1}. Lower Paleozoic); (d) Lithostratigraphic framework with conodont biostratigraphy^[25] and sample positions of the Shangsi section

本次研究的晚二叠世吴家坪阶沉积序列总体厚度约 85.7 m, 由吴家坪组 (0~55.6 m) 和大隆组下部 (55.6~85.7 m) 组成。吴家坪组底部为厚约 2 m 的王坡页岩, 与下伏茅口组具有不整合接触 (图 2a), 与上覆大隆组为整合接触 (图 2d)。吴家坪组下部发育生屑泥晶灰岩 (图 2g), 向上则逐渐硅化 (图 2h), 中上部则发育灰色硅质结核灰岩, 可见典型硅质条带 (图 2b) 和硅质团块 (图 2c)。大隆组下部可以分为 3 个岩性组合, 由下至上分别为深灰色硅质结核灰岩、薄层灰黑色富有机质泥灰岩及深灰色泥晶灰岩 (图 2e, i), 可见大量菊石等深水标志化石 (图 2f)。上寺剖面吴家坪阶整体岩石学特征表明该剖面沉积序列

向上持续变深。

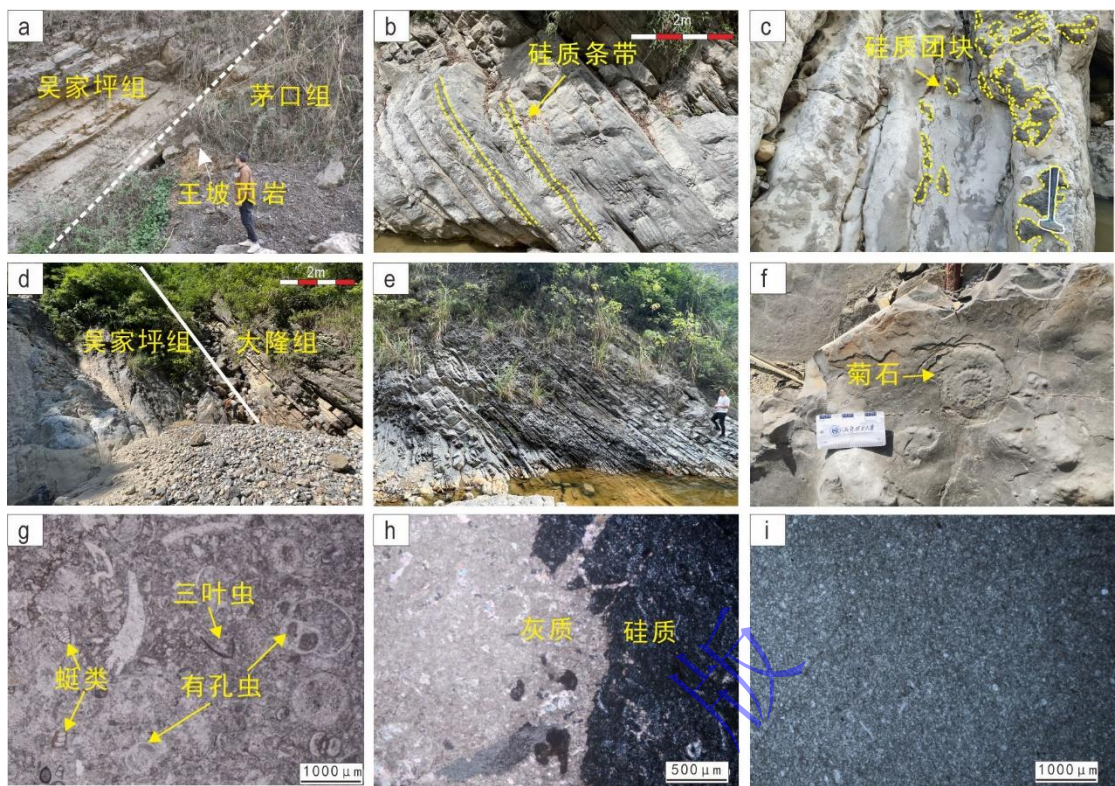


图 2 上寺剖面地层界线及岩石学特征

(a) 吴家坪组—茅口组地层界线; (b) 硅质条带, 吴家坪组; (c) 硅质团块, 吴家坪组; (d) 吴家坪组—大隆组地层界线; (e) 薄层富有机质泥灰岩, 大隆组; (f) 菊石, 大隆组; (g) 生物碎屑灰岩, 吴家坪组; (h) 硅质灰岩, 吴家坪组; (i) 泥晶灰岩, 大隆组

Fig.2 Stratigraphic boundary and petrological characteristics of the Shangsi section

(a) stratigraphic boundary between the Wuchiaping Formation and Maokou Formation; (b) siliceous strip, Wuchiaping Formation; (c) siliceous mass, Wuchiaping Formation; (d) stratigraphy boundary between the Wuchiaping Formation and Talung Formation; (e) thin layer organic-rich mudstone and limestone, Talung Formation; (f) ammonoid, Talung Formation; (g) bioclastic limestone, Wujiaping Formation; (h) micritic limestone, Talung Formation

2 样品及实验方法

在上寺剖面的吴家坪组—大隆组下部系统采集碳酸盐岩样品共计 38 件, 其中来自吴家坪组的样品为 23 件, 来自大隆组下部的样品为 15 件, 具体采样层位见图 1c。本研究采集的样品均尽量避开风化、发育次生裂隙和脉体, 为岩性均匀的新鲜岩石部分。称取样品约 50 g, 使用去离子水在超声仪中清洗干净。随后烘干样品, 碎至 200 目以下。最终将所有样品分为两个部分, 分别用于 (1) 碳氧同位素分析和 (2) 碳酸盐岩主微量元素分析。

2.1 碳氧同位素分析

碳氧同位素分析在南京宏创勘探技术服务公司完成。具体实验流程是将碳酸盐粉末装入 12 mL 圆底硼硅酸盐容器中, 置于 72°C 恒温样品盘与无水磷酸反应, 以氦气为载体将萃

取的 CO₂送入稳定同位素质谱仪, 单个样品累计吹扫 10 次。使用四种国标 (GBW04405、GBW04406、GBW04416 和 GBW04417) 对样品进行校准。执行 VPDB 标准, $\delta^{13}\text{C}_{\text{carb}}$ 的标准偏差优于 0.01‰。所有样品碳氧同位素数据可见附表 1。

2.2 主微量元素分析

碳酸盐岩的微量元素地球化学分析在广州澳实矿物实验室完成。将 0.05 g 样品粉末用 1 M 乙酸在 30 °C 的超声波水浴中溶解 30 分钟, 然后将溶液在室温下放置 12 h。将溶液离心并清洗 3 次, 将残余物烘干并称重以计算溶解百分比。随后将上清液在 120°C 下蒸发至接近干燥, 并重新溶解在 0.2 M HNO₃ 中。微量元素分析在 American PE 5300V 上进行。分析过程采用国家标准 GBW07314、GBW07315、GBW07316 和美国地质调查局玄武岩标准物质 6BHVO-2 作质量监控, 大部分元素结果相对误差小于 5%。所有样品的主微量元素数据可见附表 2。

3 结果

根据指标垂向上的系统变化, 可以将研究序列分成三个阶段。本次研究测定的 $\delta^{13}\text{C}_{\text{carb}}$ 值介于 +1.3‰~+5.1‰, 平均值为 +3.7‰ (图 3)。阶段 I, $\delta^{13}\text{C}_{\text{carb}}$ 值从 +2.1‰ 上升并稳定在较高值平台 (平均值为 +4.4‰); 阶段 II, $\delta^{13}\text{C}_{\text{carb}}$ 值逐步下降, 平均值为 +3.5‰; 阶段 III, $\delta^{13}\text{C}_{\text{carb}}$ 值总体稳定在 +3.0‰ 左右。

通常当海水处于氧化环境, Ce (III) 会转化为 Ce (IV), 并以可溶性离子的形式进入水柱^[41-42], 然后由氧化锰和氢氧化物颗粒从水柱中除去^[43-44]。因此, 浅海碳酸盐岩中 Ce 异常指标 (Ce^*) 可以示踪古海水的氧化还原程度^[45-46]。 Ce^* 的计算采用 Lawrence *et al.*^[47] 提出的公式, 可以避免传统 Ce 异常计算公式中由于海水中 La 富集过多而导致的 Ce 异常值偏差:

$$\text{Ce/Ce}^* = \text{Ce}_N / (\text{Pr}_N^2 / \text{Nd}_N) \quad (1)$$

式中: X_N (X 为式中的元素) 为 PASS 标准化后样品的含量。本次研究样品的 Ce^* 变化范围为 0.43~1.42, 平均值为 0.78。根据 Ce^* 垂向上的系统变化, 可以将研究序列分为 3 个阶段。在阶段 I (吴家坪早期), Ce^* 相对稳定在 0.65 的较低值区域。在阶段 II (吴家坪中期), Ce^* 呈上升趋势并达到最大值 1.42。随后在阶段 III (吴家坪晚期), Ce^* 下降并稳定在 0.81 附近 (图 3)。

此外, 本次研究还选取 Th、Sc、Y/Ho、Mn/Sr 等一系列指标来判别 Ce^* 是受到非氧化还原因素的干扰。Th 值整体范围为 0.03~2.64, 平均值为 0.38 (图 3); Sc 值整体范围为

0.10~4.20 平均值为 0.63 (图 3); Y/Ho 比值整体范围为 28.42~60.00, 平均值为 41.39 (图 3); Mn/Sr 比值整体范围为 0.02~0.58, 平均值为 0.11 (图 3)。

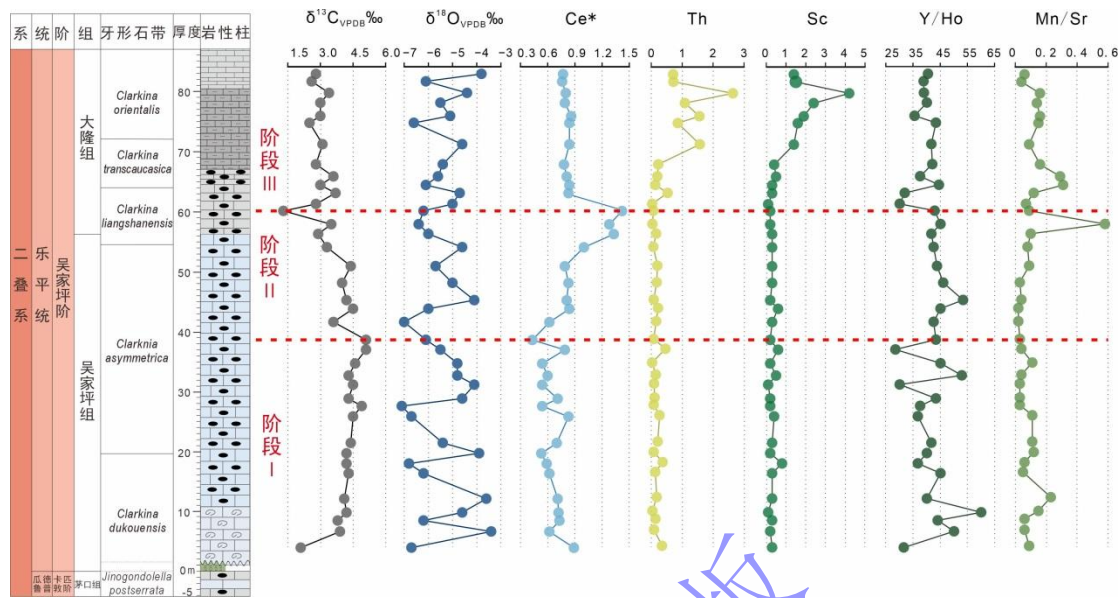


图 3 上寺剖面 $\delta^{13}\text{C}_{\text{carb}}$, $\delta^{18}\text{O}_{\text{carb}}$, Ce^* (铈异常), Th, Sc, Y/Ho, Mn/Sr 变化 (岩性图例与图 1 相同, 水平虚线表示区间划分)

Fig.3 Variations of $\delta^{13}\text{C}_{\text{carb}}$ (carbon isotopes of carbonate), $\delta^{18}\text{O}_{\text{carb}}$ (oxygen isotopes of carbonate), Ce^* (Ce anomaly), Th, Sc, Y/Ho, and Mn/Sr in the Shangsi section (the lithology legends are the same as in Fig.1, horizontal dashed lines represent interval divisions)

4 讨论

4.1 数据评估

4.1.1 碳同位素评估

海相碳酸盐岩碳同位素组成是重建古环境等最有效的手段^[48-49], 然而成岩作用会显著改变岩石中的原始地球化学信号, 因此为了获得更准确的地球化学信息, 我们需要排除可能存在的成岩作用影响, 通常可以借助岩石学手段和样品地球化学特征两个方法判别。本次研究区位于台地—盆地过渡带的环境, 剖面上没有明显的暴露标志; 镜下观察岩石薄片均为均一的泥晶结构, 因此初步判断样品未受到显著的成岩作用影响。

成岩作用会对碳酸盐岩中氧同位素组成造成显著影响^[50], 由此碳氧同位素的正相关性可以用于指示成岩作用^[7,51]。此外, 样品中 $\delta^{18}\text{O}$ 含量低于 -8‰ 也被认为是受到了成岩作用影响^[48]。本次研究所有样品 $\delta^{18}\text{O}$ 都高于 -8‰ 且与 $\delta^{13}\text{C}_{\text{carb}}$ 的相关性较弱 ($R^2=0.01$; 图 4a), 因此, 可以认为样品并未受显著成岩作用改造。碳酸盐岩在成岩作用的过程中常常会表现出锰的富集和锶的损耗^[48], 因此 Mn/Sr 比值与 $\delta^{13}\text{C}_{\text{carb}}$ 之间较差的相关性 ($R^2=0.02$; 图 4b), 强有力地证明样品保存了近乎原始的 $\delta^{13}\text{C}_{\text{carb}}$ 值。

4.1.2 Ce 异常评估

碳酸盐岩 Ce^* 可能会受到陆源碎屑输入和成岩作用等因素的影响^[52-53]，在利用碳酸盐岩 Ce^* 示踪海水氧化还原状态之前，应首先排除上述因素的影响。

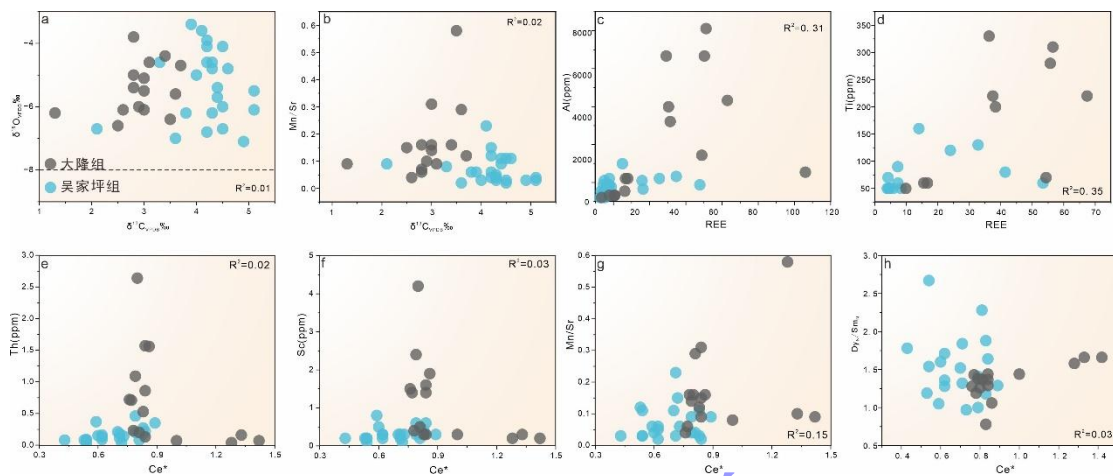


图 4 二元指标协变图

(a) $\delta^{13}\text{C}_{\text{carb}}$ 与 $\delta^{18}\text{O}_{\text{carb}}$ 协变图; (b) $\delta^{13}\text{C}_{\text{carb}}$ 与 Mn/Sr 协变图; (c) Al 与 REE 协变图; (d) Ti 与 REE 协变图; (e) Th 与 Ce^* 协变图; (f) Sc 与 Ce^* 协变图; (g) Mn/Sr 与 Ce^* 协变图; (h) Dy_N/Sm_N 与 Ce^* 协变图

Fig.4 Binary index crossplots

(a) crossplot of $\delta^{13}\text{C}_{\text{carb}}$ and $\delta^{18}\text{O}_{\text{carb}}$; (b) crossplot of $\delta^{13}\text{C}_{\text{carb}}$ and Mn/Sr; (c) crossplot of Al and Rare Earth Elements (REE); (d) crossplot of Ti and REE; (e) crossplot of Th and Ce^* ; (f) crossplot of Sc and Ce^* ; (g) crossplot of Mn/Sr and Ce^* ; (h) crossplot of Dy_N/Sm_N and Ce^*

由于 Y 与 Ho 在海水中的表面络合行为不同，Y/Ho 可以用来指示不同的水体类型^[54]。一般可以认为 Y/Ho 比值大于 36 时，碳酸盐岩样品属于海水沉积，可以反映海洋 REE（稀土元素；Rare Earth Element）信号^[26-27]。本研究中大部分样品的 Y/Ho 值大于 36，可以认为本次研究样品的 REE 值基本反映原始海水信息。碳酸盐岩形成过程中的陆源碎屑会影响碳酸盐岩的 REE 特征，影响对原始海水的氧化还原状态的判别^[26]。本研究中 Al 和 Ti 等不溶性元素的含量较低，与 REE 的相关系数分别为 0.31 和 0.35（图 4c, d），表明本次研究样品的 REE 值未受到显著成岩作用影响。同时，通过不溶性元素 Th 和 Sc 的富集程度可以判别碳酸盐岩中 Ce^* 受到陆源输入的影响程度^[55]。本研究中 Th 和 Sc 的含量均较低，且与 Ce^* 之间的相关系数为 0.02 和 0.03（图 4e, f），未显示出明显的相关性，表明吴家坪组 Ce^* 基本未受陆源碎屑物质输入的影响，可以反映当时的海水信息。

此外，后期成岩流体改造也会对碳酸盐岩 Ce^* 值造成影响^[56]，导致碳酸盐岩中 Mn 含量的增高和 Sr 含量的降低。因此，Mn/Sr 值也可用来作为可靠的指标判断原岩是否受到成岩流体的影响。本研究中 Mn/Sr 值皆小于 1.0，且与 Ce^* 的相关系数为 0.15（图 4g），说明成岩作用影响较小。碳酸盐岩中 Dy_N/Sm_N 值可指示成岩过程中选择性吸收成岩流体中的中稀土元素的程度^[57]，本研究中 Dy_N/Sm_N 值与 Ce^* 值相关系数为 0.03（图 4h），指示微弱的

后期成岩作用。

综合上述评估，本研究获得的 Ce^* 值基本未受到陆源碎屑物质输入和成岩作用等因素的影响，可以反映原始海水信息。

4.2 吴家坪期碳同位素偏移事件

碳同位素的波动主要受到碳源（如火山去气和有机物氧化等）和碳汇（如有机碳和无机碳埋藏等）的动态变化控制^[58-59]。通常碳同位素的正偏移被认为与有机碳的大量埋藏有关，生物固碳过程中优先使用环境中的 ^{12}C ，会导致有机碳埋藏量的增加，水体中溶解无机碳的 $\delta^{13}\text{C}$ 值会升高^[58,60]。碳同位素的负偏移则是由于轻碳的大量输入造成，可能原因包括火山喷发^[61]、甲烷水合物的释放^[62]及有机质氧化^[58]等。

地质历史时期出现过多次大规模的碳循环扰动事件，均与当时有机碳埋藏或氧化密切相关。例如晚埃迪卡拉世的 Shuram 事件^[63-64]被认为是有机质氧化造成的碳同位素负偏，晚寒武世 SPICE 事件^[65-66]通常被认为缺氧海水导致有机碳埋藏增强从而造成的碳同位素正偏，早石炭世 TICE 事件^[67-68]普遍认为是植物扩张导致有机碳大量埋藏有关。本次研究的上寺剖面在晚二叠世吴家坪期位于与广海连通的浅水到深水之间的过渡带，能够与广海进行通畅交换。这一时期碳同位素呈现为先正偏后负偏，表明该时期具有显著的碳循环波动。

上寺剖面在阶段 I 碳同位素的正偏幅度约为 $3.0\text{\textperthousand}$ ，随后保持在一个稳定的高值平台（平均值为 $+4.4\text{\textperthousand}$ ）。这一正偏趋势在华南滇黔桂地区的合山剖面^[7]，南秦岭的西口剖面^[69]，亚美尼亚的 Scovetashan 剖面^[70]，伊朗的 Abadeh 剖面^[71]和 Shahreza 剖面^[72]均可观察到。通常随着大规模的碳循环波动，有机碳和无机碳同位素组成变化通常呈现一致性，在澳大利亚悉尼盆地^[3]，华南 ZK15916 钻孔^[8]和南极的 Portal 山剖面^[73]的有机碳同位素变化也同样响应了这一正偏现象（图 5）。吴家坪早期的碳同位素正偏可能与有机碳大量埋藏密切相关^[74-75]，对应于气候冷却和高纬度 P4 冰川的形成。

阶段 II，上寺剖面碳同位素呈现显著负偏，负偏幅度达到 $3.8\text{\textperthousand}$ 。该负偏趋势在华南的合山剖面^[7]，南秦岭的西口剖面^[69]，亚美尼亚的 Scovetashan 剖面^[70]，伊朗的 Abadeh 剖面^[71]和 Shahreza 剖面^[72]的无机碳同位素记录及澳大利亚的悉尼盆地^[3]，华南 ZK15916 钻孔^[8]和南极 Portal 山剖面^[73]的有机碳同位素记录中均可观察到（图 5）。尽管不同的地理环境导致偏移幅度有所差异，但结合同期生物地层和旋回地层，表明吴家坪中期的碳同位素负偏可以在区域和全球地层中进行对比，该碳同位素负偏可能代表了晚古生代冰期末期的碳循环扰动^[7,76]，其对应于气候变暖和 P4 冰期的消融。

基于汇总全球吴家坪期碳同位素数据分析，可以认为不同沉积环境下会对碳同位素的

偏移幅度造成潜在影响。位于台地的合山剖面正偏幅度为 2.1‰，位于斜坡的上寺剖面正偏幅度为 3.0‰；合山剖面负偏移幅度为 5.2‰，上寺剖面的负偏移幅度为 3.8‰。前者的 $\delta^{13}\text{C}$ 值正偏移幅度低于后者的 $\delta^{13}\text{C}$ 值，负偏移幅度大于后者，这可能与陆源输入和有机碳降解有关。浅水台地受水动力环境和海平面变化的控制，部分有机碳可能在埋藏过程中发生耗氧降解甚至埋藏后再氧化^[77-78]，导致 $\delta^{13}\text{C}$ 值的降低。相较于斜坡，浅水台地更容易受到陆源输入物质的影响，陆源输入会显著改变碳酸盐岩中碳同位素，造成碳同位素显著负偏^[79]。

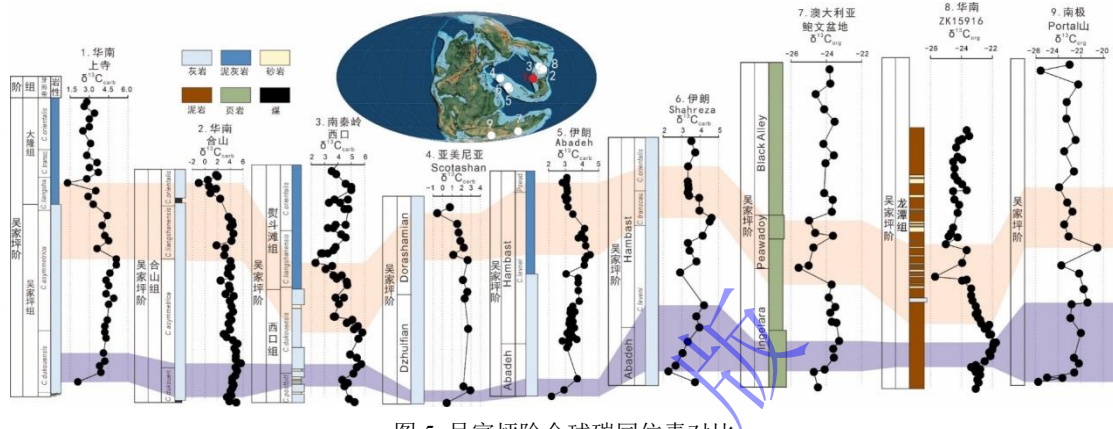


图 5 吴家坪阶全球碳同位素对比

1. 华南上寺剖面；2. 华南合山剖面^[7]；3. 南秦岭西口剖面^[69]；4. 亚美尼亚 Scotashan 剖面^[70]；5. 伊朗 Abadeh 剖面^[71]；6. 伊朗 Shahreza 剖面^[72]；7. 澳大利亚鲍文盆地^[3]；8. 华南 ZK15916 钻孔^[8]；9. 南极 Portal 山剖面^[73]

Fig.5 Global carbon isotope correlation of the Wuchiaping Formation

1. Shangsi section of South China; 2. Heshan section of South China^[7]; 3. Xikou section of South Qinling^[69]; 4. Scotashan section of Armenia^[70]; 5. Abadeh section of Iran^[71]; 6. Shahreza section of Iran^[72]; 7. Bowen basin of Australia^[3]; 8. drill Core ZK15916 of South China^[8]; 9. Portal Moutain section of Antartica^[73]

4.3 吴家坪期海洋氧化还原演化机制

晚二叠世是地质历史的关键时期，期间发生了地质历史上规模最大的二叠纪末生物大灭绝事件^[12,80]，普遍认为这一事件的启动与同时期环境变化诸如泛大陆裂解^[2,81]、大气 CO₂ 的持续升高^[82-83]、基默里地块北移^[84-85]、晚古生代冰期的结束^[3,86]、热带大陆的干旱化^[87-88]、西伯利亚大火成岩省的活动^[5,13]等有紧密联系。已有研究主要聚焦于二叠纪—三叠纪之交生物与环境之间的相互作用，对于晚二叠世早期浅海环境变化与生物响应之间的具体联系仍有待进一步探究。

瓜德鲁普末期生物灭绝事件造成了生物多样性的大幅度降低^[3,22]，峨眉山大火成岩省被认为是触发该灭绝事件的重要因素之一^[13,89-90]。峨眉山大火成岩省喷发后的基性岩风化作用是二氧化碳消耗和全球变冷的重要机制，随着二氧化碳的持续消耗及玄武岩风化的不断增强^[3,82]，碳同位素表现出正偏趋势响应了有机碳埋藏增强和气候变冷^[3,86]。进入阶段图 1（吴家坪早期）（图 6a），火山活动和玄武岩风化带来的营养物质刺激了初级生产力的提

高，生物光合作用产生氧气，促进了生物复苏和有机碳埋藏，海洋生态系统开始逐渐恢复^[91-92]。同时，气候变冷造成洋流循环加剧，强烈的上升流促进表层海水和底层海水交换，海水含氧量逐渐增加，相比与瓜德鲁普末期的海洋严重缺氧硫化，吴家坪早期海洋已转变为贫氧—氧化环境。

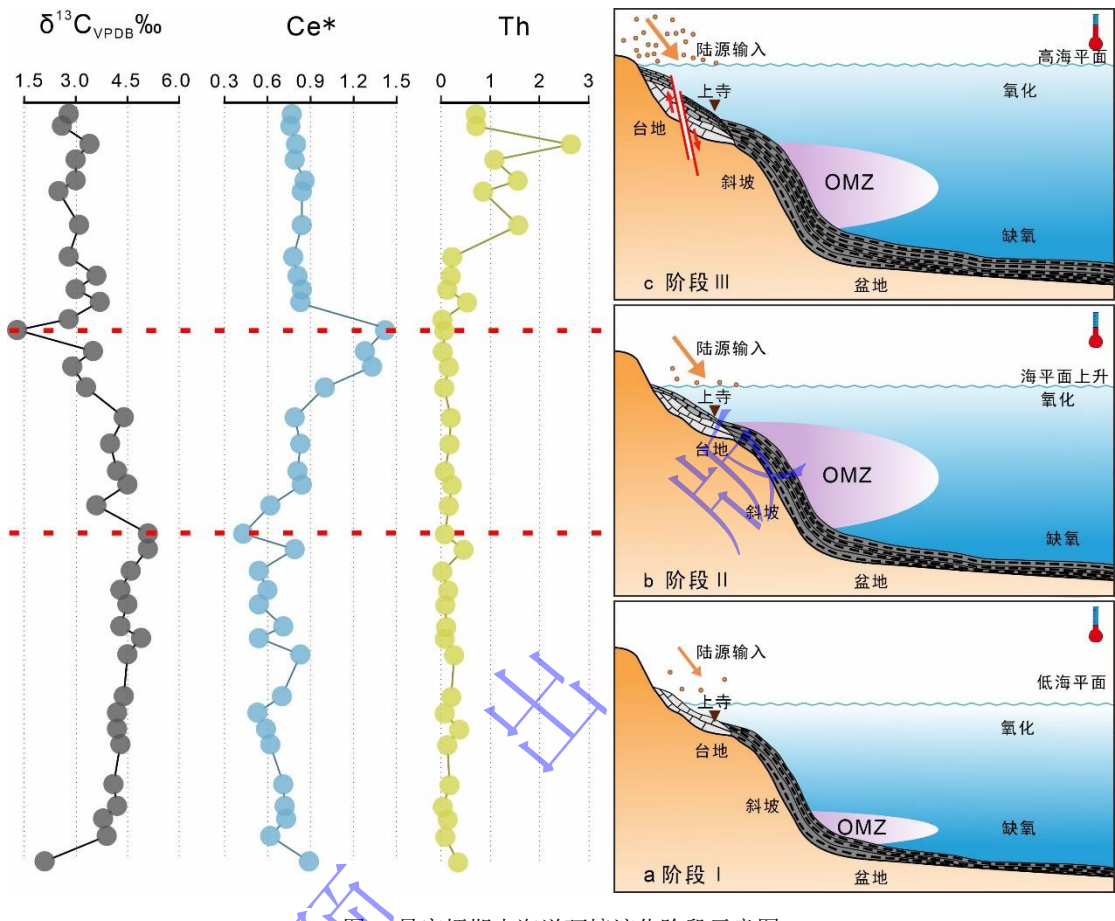


图 6 吴家坪期古海洋环境演化阶段示意图

Fig.6 Schematic diagram illustrating the Wuchiapingian paleoenvironmental evolution

阶段II（吴家坪中期）（图6b），基于牙形刺氧同位素重建的古温度曲线和陆地土壤化学元素计算的大陆风化指标^[3,93-94]指示吴家坪中期温度升高，气候变暖一方面导致的高纬度冰川融化，造成全球海平面逐渐上升^[36]，上寺剖面吴家坪组浅灰色中层硅质结核灰岩到大隆组深灰色薄层硅质结核灰岩的岩性转变很好地响应了沉积水体变深；另一方面由于气候变暖，海水氧溶解量降低，海洋循环减缓，通风减弱，加剧了水体分层。这些因素共同导致了最小含氧带（OMZ）的显著扩张，吴家坪中期海洋逐渐缺氧，该缺氧事件也与同期已报道的海水 $\delta^{238}\text{U}$ 和 $\delta^{34}\text{S}$ 指标变化相吻合^[95-96]。

阶段III（吴家坪晚期）（图6c），受扬子北缘伸展裂解和勉略洋俯冲的构造活动影响，上扬子形成“台—盆相间”的构造—沉积分异格局^[97-99]，陆源输入相对增强。该时期随着晚古生代冰期彻底结束，兼之构造活动影响，这些因素共同导致沉积水体进一步加深，上

寺剖面大隆组地层由深灰色硅质结核灰岩转变为黑色富有机质泥灰岩。该阶段碳酸盐岩 Ce^* 值总体呈现负异常，但整体相较于阶段 I 仍表现为更还原的特征。

5 结论

(1) 根据碳酸盐岩 Ce 异常指标曲线的系统变化，可以将晚二叠世吴家坪期浅海氧化还原条件演化分为三个阶段：①阶段 I (吴家坪早期)，海水整体趋于贫氧—氧化；②阶段 II (吴家坪中期)，海水转变为强烈缺氧；③阶段 III (吴家坪晚期)，海水性质相较于阶段 I 更为还原。

(2) 碳同位素在吴家坪早期呈现显著正偏，随后吴家坪中期又出现明显的负偏，这一碳同位素变化规律在全球不同地区均可以观察到。碳同位素由正偏到负偏的变化对应于海水由弱氧化转变为缺氧条件，表明碳循环扰动事件与氧化还原环境转变密切相关。

(3) 吴家坪早期，初级生产力逐渐恢复和海洋通风加强导致海水含氧量增加，海洋处于贫氧—氧化环境；吴家坪中期，气候变暖和海平面上升共同促进最小含氧带的扩张，海洋显著缺氧；吴家坪晚期，构造运动导致沉积水体进一步加深，海水相对缺氧。

参考文献(References)

- [1] 杜远生, 殷鸿福, 王治平. 秦岭造山带晚加里东—早海西期的盆地格局与构造演化[J]. 地球科学: 中国地质大学学报, 1997, 22 (4): 401-405, 410. [Du Yuansheng, Yin Hongfu, Wang Zhiping. The Late Caledonian-Early Hercynian basin's framework and tectonic evolution of Qingling orogenic belt[J]. Earth Science: Journal of China University of Geosciences, 1997, 22(4): 401-405, 410.]
- [2] Muttoni G, Gaetani M, Kent D V, et al. Opening of the Neo-Tethys ocean and the Pangea B to Pangea a transformation during the Permian[J]. GeoArabia, 2009, 14(4): 17-48.
- [3] Fielding C R, Frank T D, Birgenheier L P. A revised, Late Palaeozoic glacial time-space framework for eastern Australia, and comparisons with other regions and events[J]. Earth-Science Reviews, 2023, 236: 104263.
- [4] Liu C, Jarochowska E, Du Y S, et al. Stratigraphical and $\delta^{13}\text{C}$ records of Permo-Carboniferous platform carbonates, South China: Responses to Late Paleozoic icehouse climate and icehouse–greenhouse transition[J]. Palaeogeography, Palaeoclimatology, Palaeoecology, 2017, 474: 113-129.
- [5] Renne P R, Basu A R. Rapid eruption of the siberian traps flood basalts at the permo-Triassic boundary[J]. Science, 1991, 253(5016): 176-179.
- [6] Burgess S D, Bowring S A. High-precision geochronology confirms voluminous magmatism before, during, and after Earth's most severe extinction[J]. Science Advances, 2015, 1(7): e1500470.
- [7] Shen S Z, Cao C Q, Zhang H, et al. High-resolution $\delta^{13}\text{C}_{\text{carb}}$ chemostratigraphy from Latest Guadalupian through Earliest Triassic in South China and Iran[J]. Earth and Planetary Science Letters, 2013, 375: 156-165.
- [8] Yang J H, Cawood P A, Yuan X P, et al. Enhanced denudation of the emeishan large igneous province and precipitation forcing in the Late Permian[J]. Journal of Geophysical Research: Solid Earth, 2023, 128(12): e2023JB027430.
- [9] Wu Y Y, Chu D L, Tong J N, et al. Six-fold increase of atmospheric $p\text{CO}_2$ during the Permian–Triassic mass extinction[J]. Nature Communications, 2021, 12(1): 2137.

- [10] Chen C S, Qin S F, Wang Y P, et al. High temperature methane emissions from Large Igneous Provinces as contributors to Late Permian mass extinctions[J]. *Nature Communications*, 2022, 13(1): 6893.
- [11] Shen S Z, Crowley J L, Wang Y, et al. Calibrating the end-Permian mass extinction[J]. *Science*, 2011, 334(6061): 1367-1372.
- [12] Sun Y D, Farnsworth A, Joachimski M M, et al. Mega El Niño instigated the end-Permian mass extinction[J]. *Science*, 2024, 385(6714): 1189-1195.
- [13] 陈军, 徐义刚. 二叠纪大火成岩省的环境与生物效应: 进展与前瞻[J]. 矿物岩石地球化学通报, 2017, 36 (3) : 374-393.
[Chen Jun, Xu Yigang. Permian large igneous provinces and their impact on paleoenvironment and biodiversity: Progresses and perspectives[J]. *Bulletin of Mineralogy, Petrology and Geochemistry*, 2017, 36(3): 374-393.]
- [14] 沈树忠, 张华. 什么引起五次生物大灭绝? [J]. 科学通报, 2017, 62(11): 1119-1135. [Shen Shuzhong, Zhang Hua. What caused the five mass extinctions? [J]. *Chinese Science Bulletin*, 2017, 62(11): 1119-1135.]
- [15] Dahl T W, Boyle R A, Canfield D E, et al. Uranium isotopes distinguish two geochemically distinct stages during the later Cambrian SPICE event[J]. *Earth and Planetary Science Letters*, 2014, 401: 313-326.
- [16] Saltzman M R, Edwards C T, Adrain J M, et al. Persistent oceanic anoxia and elevated extinction rates separate the Cambrian and Ordovician radiations[J]. *Geology*, 2015, 43(9): 807-810.
- [17] Liu M, Chen D Z, Jiang L, et al. Oceanic anoxia and extinction in the latest Ordovician[J]. *Earth and Planetary Science Letters*, 2022, 588: 117553.
- [18] Zheng W, Gilleadeau G J, Algeo T J, et al. Mercury isotope evidence for recurrent photic-zone euxinia triggered by enhanced terrestrial nutrient inputs during the Late Devonian mass extinction[J]. *Earth and Planetary Science Letters*, 2023, 613: 118175.
- [19] Rong J Y, Harper D A T. A global synthesis of the latest Ordovician Hirnantian brachiopod faunas[J]. *Earth and Environmental Science Transactions of the Royal Society of Edinburgh*, 1988, 79(4): 383-402.
- [20] Méhay S, Keller C E, Bernasconi S M, et al. A volcanic CO₂ pulse triggered the Cretaceous Oceanic Anoxic Event 1a and a biocalcification crisis[J]. *Geology*, 2009, 37(9): 819-822.
- [21] Yang J H, Cawood P A, Du Y S, et al. Early Wuchiapingian cooling linked to Emeishan basaltic weathering? [J]. *Earth and Planetary Science Letters*, 2018, 492: 102-111.
- [22] 沈树忠, 张华, 张以春, 等. 中国二叠纪综合地层和时间框架[J]. 中国科学 (D辑) : 地球科学, 2019, 49 (1) : 160-193. [Shen Shuzhong, Zhang Hua, Zhang Yichun, et al. Permian integrative stratigraphy and timescale of China[J]. *Scientia Sinica (Seri. D): Earth Sciences*, 2019, 49(1): 160-193.]
- [23] Yuan D X, Shen S Z, Henderson C M. Revised Wuchiapingian conodont taxonomy and succession of South China[J]. *Journal of Paleontology*, 2017, 91(6): 1199-1219.
- [24] 金玉玕, 沈树忠, Henderson C M, 等. 瓜德鲁普统 (Guadalupian) —— 乐平统 (Lopingian) 全球界线层型剖面和点 (GSSP) [J]. 地层学杂志, 2007, 31 (1) : 1-13. [Jin Yugan, Shen Shuzhong, Henderson C M, et al. The global stratotype section and point (GSSP) for the boundary between the Guadalupian and Lopingian series (Permian)[J]. *Journal of Stratigraphy*, 2007, 31(1): 1-13.]
- [25] Yuan D X, Shen S Z, Henderson C M, et al. Integrative timescale for the Lopingian (Late Permian): A review and update from Shangsi, South China[J]. *Earth-Science Reviews*, 2019, 188: 190-209.
- [26] Ling H F, Chen X, Li D, et al. Cerium anomaly variations in Ediacaran-earliest Cambrian carbonates from the Yangtze Gorges area, South China: Implications for oxygenation of coeval shallow seawater[J]. *Precambrian Research*, 2013, 225: 110-127.
- [27] Tostevin R, Wood R A, Shields G A, et al. Low-oxygen waters limited habitable space for early animals[J]. *Nature Communications*, 2016, 7: 12818.
- [28] Takahashi S, Yamasaki S I, Ogawa Y, et al. Bioessential element-depleted ocean following the euxinic maximum of the end-Permian mass extinction[J]. *Earth and Planetary Science Letters*, 2014, 393: 94-104.
- [29] 陈知, 陈波. 三峡地区埃迪卡拉纪的浅海氧化还原环境变化: 来自碳酸盐岩 Ce 异常的证据[J]. 地层学杂志, 2022, 46 (2) : 109-117. [Chen Zhi, Chen Bo. Ediacaran shallow-marine redox conditions in the Yangtze Gorges area: Evidence from carbonate cerium anomalies[J]. *Journal of Stratigraphy*, 2022, 46(2): 109-117.]

- [30] Scotese C R. An atlas of Phanerozoic paleogeographic maps: The seas come in and the seas go out[J]. *Annual Review of Earth and Planetary Sciences*, 2021, 49: 679-728.
- [31] Hou Z S, Fan J X, Henderson C M, et al. Dynamic palaeogeographic reconstructions of the Wuchiapingian Stage (Lopingian, Late Permian) for the South China Block[J]. *Palaeogeography, Palaeoclimatology, Palaeoecology*, 2020, 546: 109667.
- [32] 殷鸿福, 吴顺宝, 杜远生, 等. 华南是特提斯多岛洋体系的一部分[J]. 地球科学: 中国地质大学学报, 1999, 24 (1) : 1-12. [Yin Hongfu, Wu Shunbao, Du Yuansheng, et al. South China defined as part of Tethyan archipelagic ocean system[J]. *Earth Science: Journal of China University of Geosciences*, 1999, 24(1): 1-12.]
- [33] Rees W E. Globalization and sustainability: Conflict or convergence?[J]. *Bulletin of Science, Technology & Society*, 2002, 22(4): 249-268.
- [34] Huang H, Huyskens M H, Yin Q Z, et al. Eruptive tempo of Emeishan large igneous province, southwestern China and northern Vietnam: Relations to biotic crises and paleoclimate changes around the Guadalupian-Lopingian boundary[J]. *Geology*, 2022, 50(9): 1083-1087.
- [35] 杨帅, 陈安清, 张玺华, 等. 四川盆地二叠纪栖霞—茅口期古地理格局转换及勘探启示[J]. *沉积学报*, 2021, 39 (6) : 1466-1477. [Yang Shuai, Chen Anqing, Zhang Xihua, et al. Paleogeographic transition of the Permian Chihsia-Maokou Period in the Sichuan Basin and indications for oil-gas exploration[J]. *Acta Sedimentologica Sinica*, 2021, 39(6): 1466-1477.]
- [36] Haq B U, Schutter S R. A chronology of Paleozoic sea-level changes[J]. *Science*, 2008, 322(5898): 64-68.
- [37] 杜远生, 盛吉虎, 顾松竹. 南秦岭勉略构造混杂岩带非史密斯地层系统和地层格架[J]. 地质论评, 1999, 45 (6) : 563-570. [Du Yuansheng, Sheng Jihu, Gu Songzhu. Stratigraphic system and framework of non-smith strata in Mianxian-Lüeyang tectonic melange belt, South Qinling mountains[J]. *Geological Review*, 1999, 45(6): 563-570.]
- [38] 张超. 华南晚二叠世层序—古地理与聚煤规律研究[D]. 北京: 中国矿业大学(北京), 2013: 13-22. [Zhang Chao. Sequence-palaeogeography and coal accumulation regularities of the Late Permian in southern China[D]. Beijing: China University of Mining & Technology (Beijing), 2013: 13-22.]
- [39] 邵龙义, 张超, 闫志明, 等. 华南晚二叠世层序: 古地理及聚煤规律[J]. *古地理学报*, 2016, 18 (6) : 905-919. [Shao Longyi, Zhang Chao, Yan Zhiming, et al. Sequence-palaeogeography and coal accumulation of the Late Permian in South China[J]. *Journal of Palaeogeography*, 2016, 18(6): 905-919.]
- [40] Mundil R, Ludwig K R, Metcalfe I, et al. Age and timing of the Permian mass extinctions: U/Pb dating of closed-system zircons[J]. *Science*, 2004, 305(5691): 1760-1763.
- [41] Byrne R H, Sholkovitz E R. Marine chemistry and geochemistry of the lanthanides[J]. *Handbook on the Physics and Chemistry of Rare Earths*, 1996, 23: 497-593.
- [42] Tanaka H K M, Taira H, Uchida T, et al. Three-dimensional computational axial tomography scan of a volcano with cosmic ray muon radiography[J]. *Journal of Geophysical Research: Solid Earth*, 2010, 115(B12): B12332.
- [43] Elderfield H, Hawkesworth C J, Greaves M J, et al. Rare earth element geochemistry of oceanic ferromanganese nodules and associated sediments[J]. *Geochimica et Cosmochimica Acta*, 1981, 45(4): 513-528.
- [44] Bau M, Koschinsky A, Dulski P, et al. Comparison of the partitioning behaviours of yttrium, rare earth elements, and titanium between hydrogenetic marine ferromanganese crusts and seawater[J]. *Geochimica et Cosmochimica Acta*, 1996, 60(10): 1709-1725.
- [45] Webb G E, Kamber B S. Rare earth elements in Holocene reefal microbialites: A new shallow seawater proxy[J]. *Geochimica et Cosmochimica Acta*, 2000, 64(9): 1557-1565.
- [46] Zhang K, Shields G A. Sedimentary Ce anomalies: Secular change and implications for paleoenvironmental evolution[J]. *Earth-Science Reviews*, 2022, 229: 104015.
- [47] Lawrence M G, Greig A, Collerson K D, et al. Rare earth element and yttrium variability in South East Queensland waterways[J]. *Aquatic Geochemistry*, 2006, 12(1): 39-72.
- [48] Veizer J, Ala D, Azmy K, et al. $^{87}\text{Sr}/^{86}\text{Sr}$, $\delta^{13}\text{C}$ and $\delta^{18}\text{O}$ evolution of Phanerozoic seawater[J]. *Chemical Geology*, 1999, 161(1/2/3): 59-88.

- [49] Halverson G P, Hoffman P F, Schrag D P, et al. Toward a Neoproterozoic composite carbon-isotope record[J]. *GSA Bulletin*, 2005, 117(9/10): 1181-1207.
- [50] Banner J L, Hanson G N. Calculation of simultaneous isotopic and trace element variations during water-rock interaction with applications to carbonate diagenesis[J]. *Geochimica et Cosmochimica Acta*, 1990, 54(11): 3123-3137.
- [51] Knauth L P, Kennedy M J. The Late Precambrian greening of the Earth[J]. *Nature*, 2009, 460(7256): 728-732.
- [52] Tribouillard N, Algeo T J, Lyons T, et al. Trace metals as paleoredox and paleoproductivity proxies: An update[J]. *Chemical Geology*, 2006, 232(1/2): 12-32.
- [53] 吕苗, 鞠东澍, 王姝衡, 等. 晚泥盆世弗拉期—法门期(F-F)之交海洋氧化: 来自华南洞村剖面碳酸盐岩Ce异常证据[J]. 地层学杂志, 2024, 48(1): 77-86. [Lü Miao, Ju Dongshu, Wang Shuheng, et al. Marine oxygenation pulses during Late Devonian Frasnian-Famennian transition: Evidence from Ce anomaly record from the Dongcun section, South China[J]. *Journal of Stratigraphy*, 2024, 48(1): 77-86.]
- [54] Nozaki Y, Zhang J, Amakawa H. The fractionation between Y and Ho in the marine environment[J]. *Earth and Planetary Science Letters*, 1997, 148(1/2): 329-340.
- [55] Nothdurft L D, Webb G E, Kamber B S. Rare earth element geochemistry of Late Devonian reefal carbonates, Canning Basin, western Australia: Confirmation of a seawater REE proxy in ancient limestones[J]. *Geochimica et Cosmochimica Acta*, 2004, 68(2): 263-283.
- [56] Guido A, Mastandrea A, Tosti F, et al. Importance of rare earth element patterns in discrimination between biotic and abiotic mineralization[M]//Reitner J, Quéric N V, Arp G. *Advances in stromatolite geobiology*. Berlin, Heidelberg: Springer, 2011: 453-462.
- [57] Shields G, Stille P. Diagenetic constraints on the use of cerium anomalies as palaeoseawater redox proxies: An isotopic and REE study of Cambrian phosphorites[J]. *Chemical Geology*, 2001, 175(1/2): 29-48.
- [58] Kump L R, Arthur M A. Interpreting carbon-isotope excursions: Carbonates and organic matter[J]. *Chemical Geology*, 1999, 161(1/2/3): 181-198.
- [59] Canfield D E, Kump L R. Carbon cycle makeover[J]. *Science*, 2013, 339(6119): 533-534.
- [60] Hayes J M, Strauss H, Kaufman A J. The abundance of ^{13}C in marine organic matter and isotopic fractionation in the global biogeochemical cycle of carbon during the past 800 Ma[J]. *Chemical Geology*, 1999, 161(1/2/3): 103-125.
- [61] Grard A, François L M, Dessert C, et al. Basaltic volcanism and mass extinction at the Permo-Triassic boundary: Environmental impact and modeling of the global carbon cycle[J]. *Earth and Planetary Science Letters*, 2005, 234(1/2): 207-221.
- [62] Dickens G R, O'Neil J R, Rea D K, et al. Dissociation of oceanic methane hydrate as a cause of the carbon isotope excursion at the end of the Paleocene[J]. *Paleoceanography*, 1995, 10(6): 965-971.
- [63] Jiang L, Planavsky N, Zhao M Y, et al. Authigenic origin for a massive negative carbon isotope excursion[J]. *Geology*, 2019, 47(2): 115-118.
- [64] Cañadas F, Papineau D, Leng M J, et al. Extensive primary production promoted the recovery of the Ediacaran Shuram excursion[J]. *Nature Communications*, 2022, 13(1): 148.
- [65] Saltzman M R, Ripperdan R L, Brasier M D, et al. A global carbon isotope excursion (SPICE) during the Late Cambrian: Relation to trilobite extinctions, organic-matter burial and sea level[J]. *Palaeogeography, Palaeoclimatology, Palaeoecology*, 2000, 162(3/4): 211-223.
- [66] Xia W P, Chen A Q, Azmy K, et al. A pilot study of Upper Yangtze shallow-water carbonates of the Paibian global marine euxinia: Implications for the Late Cambrian SPICE event[J]. *Marine and Petroleum Geology*, 2023, 150: 106146.
- [67] Buggisch W, Joachimski M M, Sevastopulo G, et al. Mississippian $\delta^{13}\text{C}_{\text{carb}}$ and conodont apatite $\delta^{18}\text{O}$ records: Their relation to the Late Palaeozoic Glaciation[J]. *Palaeogeography, Palaeoclimatology, Palaeoecology*, 2008, 268(3/4): 273-292.
- [68] Yao L, Qie W K, Luo G M, et al. The TICE event: Perturbation of carbon–nitrogen cycles during the mid-Tournaisian (Early Carboniferous) greenhouse–icehouse transition[J]. *Chemical Geology*, 2015, 401: 1-14.

- [69] Cheng C, Li S Y, Xie X Y, et al. Permian carbon isotope and clay mineral records from the Xikou section, Zhen'an, Shaanxi province, central China: Climatological implications for the easternmost Paleo-Tethys[J]. *Palaeogeography, Palaeoclimatology, Palaeoecology*, 2019, 514: 407-422.
- [70] Baud A, Magaritz M, Holser W T. Permian-Triassic of the Tethys: Carbon isotope studies[J]. *Geologische Rundschau*, 1989, 78(2): 649-677.
- [71] Richoz S. Stratigraphic et variations isotopiques du carbone dans le Permien supérieur et le Trias inférieur de quelques localités de la Néotéthys (Turquie, Oman et Iran)[J]. *Mémoire de Géologie de Lausanne*, 2006, 46: 1-275.
- [72] Heydari E, Arzani N, Safaei M, et al. Ocean's response to a changing climate: Clues from variations in carbonate mineralogy across the Permian-Triassic boundary of the Shareza Section, Iran[J]. *Global and Planetary Change*, 2013, 105: 79-90.
- [73] Retallack G J, Metzger C A, Greaver T, et al. Middle-late Permian mass extinction on land[J]. *Geological Society of America Bulletin*, 2006, 118 (11/12): 1398-1411.
- [74] Birgenheier L P, Frank T D, Fielding C R, et al. Coupled carbon isotopic and sedimentological records from the Permian system of eastern Australia reveal the response of atmospheric carbon dioxide to glacial growth and decay during the Late Palaeozoic Ice Age[J]. *Palaeogeography, Palaeoclimatology, Palaeoecology*, 2010, 286(3/4): 178-193.
- [75] Frank T D, Shultz A I, Fielding C R. Acme and demise of the Late Palaeozoic ice age: A view from the southeastern margin of Gondwana[J]. *Palaeogeography, Palaeoclimatology, Palaeoecology*, 2015, 418: 176-192.
- [76] Wang P, Du Y S, Yu W C, et al. The Chemical Index of Alteration (CIA) as a proxy for climate change during glacial-interglacial transitions in Earth history[J]. *Earth-Science Reviews*, 2020, 201: 103032.
- [77] Widdicombe S, Spicer J I. Effects of ocean acidification on sediment fauna[M]//Gattuso J P, Hansson L J. *Ocean Acidification*. Oxford: Oxford University Press, 2011: 176-191.
- [78] Li D D, Zhang X L, Hu D P, et al. Evidence of a large $\delta^{13}\text{C}_{\text{carb}}$ and $\delta^{13}\text{C}_{\text{org}}$ depth gradient for deep-water anoxia during the Late Cambrian SPICE event[J]. *Geology*, 2018, 46(7): 631-634.
- [79] Berner R A. Atmospheric carbon dioxide levels over Phanerozoic time[J]. *Science*, 1990, 249(4975): 1382-1386.
- [80] 沈树忠, 张飞飞, 王文倩, 等. 深时重大生物和气候事件与全球变化: 进展与挑战[J]. 科学通报, 2024, 69 (2) : 268-285. [Shen Shuzhong, Zhang Feifei, Wang Wenqian, et al. Deep-time major biological and climatic events versus global changes: Progresses and challenges[J]. *Chinese Science Bulletin*, 2024, 69(2): 268-285.]
- [81] Santosh M, Maruyama S, Yamamoto S. The making and breaking of supercontinents: Some speculations based on superplumes, super downwelling and the role of tectosphere[J]. *Gondwana Research*, 2009, 15(1/2): 324-341.
- [82] Foster G L, Royer D L, Lunt D J. Future climate forcing potentially without precedent in the last 420 million years[J]. *Nature Communications*, 2017, 8: 14845.
- [83] Cui Y, Li M S, Van Soelen E E, et al. Massive and rapid predominantly volcanic CO₂ emission during the end-Permian mass extinction[J]. *Proceedings of the National Academy of Sciences of the United States of America*, 2021, 118(37): e2014701118.
- [84] Shen S Z, Shi G R. Latest Guadalupian brachiopods from the Guadalupian/Lopingian boundary GSSP section at Penglaitan in Laibin, Guangxi, South China and implications for the timing of the pre-Lopingian crisis[J]. *Palaeoworld*, 2009, 18(2/3): 152-161.
- [85] Wang X D, Shen S Z, Sugiyama T, et al. Late Palaeozoic corals of Tibet (Xizang) and West Yunnan, Southwest China: Successions and palaeobiogeography[J]. *Palaeogeography, Palaeoclimatology, Palaeoecology*, 2003, 191(3/4): 385-397.
- [86] Metcalfe I, Denyszyn S, Mundil R, et al. High-precision CA-IDTIMS U-Pb chronostratigraphy in the Bowen Basin, eastern Australia, calibration of deep-time climate change, super-volcanism and mass extinction[J]. *Gondwana Research*, 2024, 133: 335-347.
- [87] Boucot A J, Xu C, Scotese C R. *Phanerozoic paleoclimate: An atlas of lithologic indicators of climate*[M]. Tulsa: Society for Sedimentary Geology, 2013: 478.
- [88] 宋汉宸, 宋海军, 张仲石, 等. 古生代—中生代之交的水循环演变及驱动机制[J]. 科学通报, 2023, 68 (12) : 1501-1516. [Song Hanchen, Song Haijun, Zhang Zhongshi, et al. Evolution and driving mechanisms of water circulation during the Late Paleozoic to early Mesozoic[J]. *Chinese Science Bulletin*, 2023, 68(12): 1501-1516.]

- [89] Shellnutt J G. The Emeishan large igneous province: A synthesis[J]. Geoscience Frontiers, 2014, 5(3): 369-394.
- [90] Chen J, Xu Y G. Establishing the link between Permian volcanism and biodiversity changes: Insights from geochemical proxies[J]. Gondwana Research, 2019, 75: 68-96.
- [91] 颜佳新, 孟琦, 王夏, 等. 碳酸盐工厂与浅水碳酸盐岩台地: 研究进展与展望[J]. 古地理学报, 2019, 21 (2) : 232-253.
[Yan Jiaxin, Meng Qi, Wang Xia, et al. Carbonate factory and carbonate platform: Progress and prospects[J]. Journal of Palaeogeography (Chinese Edition), 2019, 21(2): 232-253.]
- [92] Fan J X, Shen S Z, Erwin D H, et al. A high-resolution summary of Cambrian to early Triassic marine invertebrate biodiversity[J]. Science, 2020, 367(6475): 272-277.
- [93] Chen B, Joachimski M M, Shen S Z, et al. Permian ice volume and palaeoclimate history: Oxygen isotope proxies revisited[J]. Gondwana Research, 2013, 24(1): 77-89.
- [94] Chen J, Shen S Z, Li X H, et al. High-resolution SIMS oxygen isotope analysis on conodont apatite from South China and implications for the end-Permian mass extinction[J]. Palaeogeography, Palaeoclimatology, Palaeoecology, 2016, 448: 26-38.
- [95] Wang W Q, Zhang F F, Zhang S, et al. Ecosystem responses of two Permian biocrises modulated by CO₂ emission rates[J]. Earth and Planetary Science Letters, 2023, 602: 117940.
- [96] Li P W, Huang J H, Chen M, et al. Coincident negative shifts in sulfur and carbon isotope compositions prior to the end-Permian mass extinction at Shangsi Section of Guangyuan, South China[J]. Frontiers of Earth Science in China, 2009, 3(1): 51-56.
- [97] 冯纯江, 张继庆, 官举铭. 四川盆地上二叠统沉积相及其构造控制[J]. 岩相古地理, 1988 (2) : 1-15. [Feng Chunjiang, Zhang Jiqing, Guan Juming. The Upper Permian sedimentary facies in Sichuan Basin and their tectonic controls[J]. Sedimentary Geology and Tethyan Geology, 1988(2): 1-15.]
- [98] 李维波, 李江海, 王洪浩, 等. 二叠纪古板块再造与岩相古地理特征分析[J]. 中国地质, 2015, 42 (2) : 685-694. [Li Weibo, Li Jianghai, Wang Honghao, et al. Characteristics of the reconstruction of Permian paleoplate and lithofacies paleogeography[J]. Geology in China, 2015, 42(2): 685-694.]
- [99] 陈旭, 胡明毅, 徐昌海, 等. 四川盆地开江—梁平海槽边缘二叠世长兴期台缘礁滩沉积结构及其差异性[J]. 石油与天然气地质, 2022, 43 (4) : 833-844. [Chen Xu, Hu Mingyi, Xu Changhai, et al. Sedimentary architectures of reef-shoal facies at the platform margin during Changxing times of the Late Permian around Kaijiang-Liangping trough in the Sichuan Basin and their differences[J]. Oil & Gas Geology, 2022, 43(4): 833-844.]

Reconstruction of Ocean Redox Environment During the Late Permian Wuchiapingian, Northern Margin of Upper Yangtze

YONG RuNan^{1,2}, SUN Shi^{1,2}, CHEN AnQing^{1,2}, HOU MingCai^{1,2}, LI KuiZhou^{1,2}, LI Qian^{3,4}, HUANG GuangHui^{1,2}, LI Wen^{1,2}, XIE Hao¹, CHEN HongDe^{1,2}

1. State Key Laboratory of Oil and Gas Reservoir Geology and Exploitation, Chengdu University of Technology, Chengdu 610059, China

2. Key Laboratory of Deep-time Geography and Environment Reconstruction and Applications of Ministry of Natural Resources, Chengdu University of Technology, Chengdu 610059, China

3. School of Environment and Resource, Southwest University of Science and Technology, Mianyang, Sichuan 621010, China

4. School of Earth Environment, University of Leeds, Leeds, UK LS2 9JT

Abstract: [Objective] Although the End-Guadalupian Extinction is not as well known as the End-Permian Extinction, it is regarded as a critical event that resulted in considerable biodiversity loss and significant

disruptions to ecosystems. Following the End-Guadalupian extinction, global biodiversity was progressively restored during the Late Permian. Despite this recovery, the intricate relationship between biological resurgence during this era and the redox conditions of palaeo-oceans is still not fully understood. [Method] The Wuchiaping Formation located in the Shangsi section of the northern margin of the Yangtze Block with high-resolution time frame constraints was selected as the research object. Petrological and sedimentary geochemical studies were employed to reconstruct the marine redox environment associated with the Wuchiaping Formation in the Late Permian. By examining the rock composition and geochemical signatures of the rock samples, we established key indicators of redox conditions (Ce^* ; Ce anomaly). Additionally, we selected several indicators, including Th, Sc, Y/Ho, and Mn/Sr, to assess whether the redox indicator was influenced by non-redox factors. [Results] The collected global carbon isotope from the Wuchiapingian of Late Permian consistently exhibited a significant positive bias in the Early Wuchiapingian, followed by a notable negative bias in the Middle Wuchiapingian changes, indicating that this carbon cycle disturbance event had a worldwide impact. Moreover, this transformation corresponds to changes in seawater redox conditions, showing a close correlation between carbon cycle disturbance events and alteration in redox environments. Through comparison of the stratigraphic framework, the disturbance was found to align with the waxing and waning of P4 glaciation. Based on the systematic changes in the Ce anomaly curve of carbonate rocks, the evolution of marine redox conditions during the Wuchiapingian of Late Permian can be divided into three stages, reflecting three distinct global shifts in climate and environmental conditions. The gradual resurgence of early organisms led to an increase in primary productivity and photosynthesis, and the cooler climate was conducive to ocean circulation and facilitated oxygen exchange, resulting in an oxygen-poor environment. As the climate gradually warmed and the Late Paleozoic Ice Age ended, the situation began to shift dramatically. The weakening of ocean ventilation, caused by alterations in temperature gradients and circulation patterns, coupled with rising sea levels contributed to the expansion of the minimum oxygen zone, consequently transforming the ocean into an anoxic environment. This shift had profound implications for marine life and the overall health of ocean ecosystems, setting the stage for significant biological upheaval in the ensuing geological periods. [Conclusion] The study developed a redox model of the shallow marine environment during the Wuchiapingian, providing insight into the interactions between various environmental factors. It highlights a significant connection between the oceanic hypoxia event and the simultaneous biological and geological tectonic activities occurring. By examining these relationships, the research enhances our understanding of how environmental factors influenced marine life and sedimentary processes during this critical period in Earth history.

Key words: Late Permian; Ce anomaly; ocean anoxia; biological recovery; Upper Yangtze